


## Article

# Applicability of Traditional Acoustic Technology for Underwater Archeology: A Case Study of Model Detection in Xiamen Bay

Xudong Fang<sup>1</sup>, Jianglong Zheng<sup>2,\*</sup>, Shengtao Zhou<sup>3</sup>, Zepeng Huang<sup>4</sup>, Boran Liu<sup>1</sup>, Ping Chen<sup>5</sup> and Jiang Xu<sup>1</sup>

<sup>1</sup> Fujian Provincial Key Laboratory of Marine Physical and Geological Processes, Third Institute of Oceanography, Ministry of Natural Resources, Xiamen 361005, China; fangxudong@tio.org.cn (X.F.); liuboran@tio.org.cn (B.L.); xujiang@tio.org.cn (J.X.)

<sup>2</sup> Shenzhen Institutes of Advanced Technology, Chinese Academy of Sciences, Shenzhen 518055, China

<sup>3</sup> Tianjin Qilan Technology Co., Ltd., Tianjin 300354, China; zhoushengtao622@163.com

<sup>4</sup> National Centre for Archeology of China, Beijing 100013, China; zp.huang@uch-china.com

<sup>5</sup> Xiamen Marine Engineering Survey, Design and Research Institute Co., Ltd., Xiamen 361005, China; chenping@tio.org.cn

\* Correspondence: jl.zheng@siat.ac.cn

## Abstract

This study addresses the applicability of conventional marine acoustic technologies for detecting non-metal artifacts. Based on the typical environment in Xiamen Bay, we evaluated the detection efficacy of common multibeam sonar, side-scan sonar, and sub-bottom profiling sonar through a controlled model experiment system. We employed ceramic artifact replicas (ranging in size from 10 to 70 cm) and incorporated acoustic parameter optimization to elucidate the applicability boundaries of different technologies. The results indicate that multibeam sonar can identify clustered targets larger than 0.5 m, but is limited in resolving small individual targets (less than 30 cm) due to terrain detail constraints. Side-scan sonar, under low-speed (less than 4 knots) and near-bottom operating conditions, effectively captures the high-intensity echo characteristics of ceramic targets, achieving a maximum effective detection range of more than 40 m. High-frequency sub-bottom profiler (94–110 kHz) offers resolution advantages for exposed artifacts, while low-frequency signals (5–15 kHz) provide theoretical support for detecting subsequently buried targets. Furthermore, the study quantifies the coupling effects of substrate type, target size, and surface roughness on acoustic responses. We propose a synergistic detection workflow comprising “multibeam initial screening—side-scan fine mapping—sub-bottom profiling validation,” which provides empirical support for the optimization and standardization of underwater archeological technologies in complex marine environments.

**Keywords:** underwater archeology; geophysical prospecting; acoustic technology; model experiments; Xiamen Bay



Academic Editors: Jian Kang and Alexander Sutin

Received: 28 June 2025

Revised: 28 August 2025

Accepted: 15 September 2025

Published: 22 September 2025

**Citation:** Fang, X.; Zheng, J.; Zhou, S.; Huang, Z.; Liu, B.; Chen, P.; Xu, J. Applicability of Traditional Acoustic Technology for Underwater Archeology: A Case Study of Model Detection in Xiamen Bay. *Acoustics* **2025**, *7*, 59. <https://doi.org/10.3390/acoustics7030059>

**Copyright:** © 2025 by the authors. Licensee MDPI, Basel, Switzerland. This article is an open access article distributed under the terms and conditions of the Creative Commons Attribution (CC BY) license (<https://creativecommons.org/licenses/by/4.0/>).

## 1. Introduction

Underwater archeological research is conducted in several stages after the comprehensive collection and analysis of historical data. These stages include regional preliminary surveys, potential area assessments, detailed investigations of key sites, and the excavation, restoration, and preservation of sites [1]. In recent years, the application of geophysical survey techniques in underwater archeology has developed into a systematic framework, demonstrating significant technological advantages and innovative potential. Compared to traditional marine geophysical surveys, underwater archeology places greater emphasis

on determining the orientation, preservation state, and burial conditions of underwater remains, thereby imposing higher demands on the interpretative accuracy and reliability of detection technologies.

Current underwater archeological survey technologies primarily encompass three major systems: acoustic, electromagnetic, and optical methods. These technologies enable the localization and characterization of archeological sites through the integration of multi-source data [2,3]. Acoustic techniques dominate the field. Imaging sonar systems, including multi-beam bathymetry, side-scan imaging, and three-dimensional imaging sonar, can provide high-resolution data on seabed morphology and the characteristics of underwater structures, revealing archeological remains such as shipwrecks that are mostly exposed or partially buried. However, they cannot detect fully buried objects. Sub-bottom profiling is an effective method for discovering buried objects on the seafloor and there are many successful cases [4–12]. The case study results show that the emission signal of the seismic source, the design of the source receiver geometry and the signal processing may directly affect the application effect of the sub-bottom profiler in underwater archeology. However, the biggest problem with sub-bottom profiler is the inefficiency of detection. Electromagnetic methods, centered around magnetometers, can be used to detect iron artifacts by identifying magnetic anomalies but limited by its probing principle. Laser and optical imaging are of great significance for the advancement of underwater archeological research since they can facilitate high-precision modeling of archeological remains [13–15]. Furthermore, the incorporation of intelligent detection platforms, artificial intelligence algorithms (e.g., YOLOv5), and the utilization of satellite measurement data have significantly expanded the scope and efficiency of underwater archeological investigations [16–19].

Conducting comprehensive geophysical surveys and assessments can reveal the structural characteristics and environmental changes in shipwreck sites, providing detailed base maps for divers and assisting researchers in exploring the formation processes of these sites. This, in turn, offers a scientific basis for the management and protection of marine archeological sites [20,21]. Additionally, the integration of geophysical techniques with other disciplines also represents an important direction for underwater archeological research, such as the combined use of sediment analysis and seismic exploration methods [22,23].

Despite significant advancements in geophysical survey technologies, challenges remain, including low identification rates for small-sized underwater artifacts, limited penetration capabilities in complex sedimentary environments (i.e., estuarine sandy bottom), and delays in real-time data processing for deep-sea sites. Future efforts should focus on further promoting multi-sensor integration, deploying autonomous platforms, optimizing machine learning algorithms, and establishing interdisciplinary collaboration mechanisms [24,25]. The key to methodological integration is approaching it from the perspective of underwater archeology.

Existing geophysical survey technologies face limitations in applicability due to the complexities of marine environments and the precision required for detecting small artifacts. While acoustic technologies dominate underwater archeology, prior studies have primarily focused on large shipwrecks or metallic artifacts [2,4]. Few address the detection limits of small (<30 cm) non-metallic relics in dynamic environments. This study bridges the gap through a series of offshore controlled model experiments. From the perspective of acoustic detection principles, both large shipwreck remains and the cargo aboard these vessels are considered anomalies relative to the naturally settled seabed sediments. These anomalies may present significant contours or characteristic features on acoustic profiles, but they can also be misinterpreted as general anomalous signals and overlooked by interpreters. Therefore, establishing an objective correlation through model deployment and field detection experiments is necessary. This study focuses on Xiamen Bay as the

experimental site. Through model deployment experiments, we systematically evaluate the detection efficacy of multibeam bathymetry systems and side-scan sonar technologies for small underwater artifacts. The aim is to provide a basis for technical optimization in underwater archeological survey. By comparing the characteristics of different marine environments and geophysical detection parameters, we propose specific detection techniques for non-metallic artifacts, such as pottery.

Section 1 outlines the role of geophysical techniques in underwater archeology and identifies knowledge gaps in detecting small non-metallic artifacts. Section 2 details the key acoustic principles of MBES, SSS, and SBP systems, and describes the controlled field experiment in Xiamen Bay, including model deployment and data acquisition protocols. Section 3 presents empirical findings on the detection capabilities of MBES (terrain anomalies), SSS (acoustic shadows/intensity), and SBP (buried target limitations) for ceramic artifacts. Section 4 analyzes operational constraints, environmental impacts (e.g., biofouling), and proposes the integrated workflow “MBES screening → SSS fine mapping → SBP validation”. Section 5 summarizes applicability boundaries of traditional acoustics and recommends future integration with AI/optical technologies.

## 2. Materials and Methods

### 2.1. Principle of MBES, SSS and SBP

It is essential to follow a systematic workflow that progresses from general surveys to detailed examinations when conducting investigations of submarine targets. This paper focuses on the workflow and key considerations involved in detecting small submarine targets using integrated acoustic technologies, exemplified by three commonly used acoustic detection systems: multibeam bathymetry, side-scan imaging, and sub-bottom profiling sonar.

Multi-beam echosounder systems (MBESs) simultaneously emit dozens to hundreds of independent acoustic beams (arranged in a fan shape) toward the seafloor using an array of transducers, and receive the echoes with another array of transducers. The area illuminated by each beam on the seafloor is referred to as the “beam footprint,” which is usually elliptical in shape. The size of the beam footprint  $S_{BPF}$  depends on the beam’s opening angle (in radians) and the water depth (in meters):

$$S_{BPF} \approx h \times \theta \quad (1)$$

The side-scan sonar (SSS) system emits a fan-shaped wide beam to the sides, with beam angles reaching several tens of degrees. The beamwidth is narrow (1–2°) along-track and wide (typically between 30 and 60°) across-track. The receiver records the intensity of backscattered signals from the seafloor, producing acoustic images. The along-track resolution is high and appears as a narrow strip. The across-track resolution decreases with increasing distance. Near-field resolution can reach the centimeter level, while far-field resolution decreases to several meters. Small targets are identified through the shadow zone, which is the area behind the target that lacks echo returns.

Sub-bottom profiler (SBP) usually emits low-frequency acoustic wave pulses (typically between 1 and 15 kHz) vertically or nearly vertically, creating a wide conical beam (with an opening angle generally ranging from 10° to 30°). The acoustic waves penetrate the seabed and are reflected at different acoustic impedance interfaces, revealing the stratigraphic structure. The beam footprint of the SBP appears circular or elliptical on the seabed, with its size increasing with water depth (similar to the formula used in MBESs). The vertical resolution is determined by the pulse length (optimally reaching 10 cm), while the horizontal resolution is constrained by the beam footprint.

MBES systems offer the advantage of high-precision three-dimensional localization of exposed small targets. However, as water depth increases, the beam footprint also

enlarges, leading to a dispersion of the target's reflected energy. An SSS can provide high-resolution imaging of the morphology of exposed small targets, but it lacks depth information and exhibits low resolution at greater distances. SBPs have the potential to detect buried targets and ascertain their depths; however, they suffer from low horizontal resolution, and current technologies face challenges in effectively identifying small targets. The spatial resolution of the three acoustic detection technologies is closely related to the beam footprint.

Theoretically, the lateral dimensions of a geological body or target must exceed the diameter of the Fresnel zone to be resolvable. In the field of seismic exploration, it is generally accepted that layers with a thickness less than  $\lambda/4$  may be inadequately imaged due to the interference effects associated with the Fresnel zone.

$$D_{Fresnel} \approx \sqrt{\lambda \times H} \quad (2)$$

In fact, all three types of acoustic detection technologies are influenced by both the beam footprint and the Fresnel zone, although the nature and extent of these influences differ. Even though MBES reduces the geometric beam footprint through a narrow beam (typically between  $0.5^\circ$  and  $2^\circ$ ), if the spacing between detection targets is smaller than the diameter of the Fresnel zone, their reflected signals can interfere with one another, preventing the system from distinguishing between adjacent targets. For isolated small targets, such as rocks or shipwreck debris, if their dimensions are smaller than the Fresnel zone, the echo energy may be “averaged out” by the surrounding seabed background, leading to a decreased signal-to-noise ratio and a lower probability of identification. These understandings are important prerequisites for obtaining high-quality raw data and data post processing.

## 2.2. Field Experiment

### 2.2.1. Experimental Sea Area

Underwater archeology is significantly restricted by three core categories of conditions: the submarine natural environment, technical adaptability, and external interference factors. The submarine natural environment is the most fundamental restricting factor. Baozhu Islet, located inside of Xiamen Bay, historically served as a crucial waterway for external communication for ancient Tong'an City. The research team selected the maritime area near Baozhu Islet as the experimental zone (as shown in Figure 1). This experimental zone is situated approximately 2000 m south of Baozhu Islet. Within the experimental zone, there exists a group of reefs with a distribution radius of about 300 m, which includes several submerged rocks. The water depth in the experimental zone ranges from 5 to 10 m, with some rocks exposed during low tide. During high tide, tidal waves from the open sea propagate towards the ends of various bays through the channels in the eastern and western waters of Xiamen; conversely, during low tide, the water generally flows in the opposite direction of the incoming tide. The maximum measured flow velocities during rising and falling tides were 71 cm/s and 66 cm/s, respectively, exhibiting a pronounced reciprocating flow characteristic due to the confinement of the waterway. The distribution of surface sediment types is relatively simple, primarily consisting of clayey silt (with silt content ranging from 60% to 75%), and the seabed exhibits good stability.



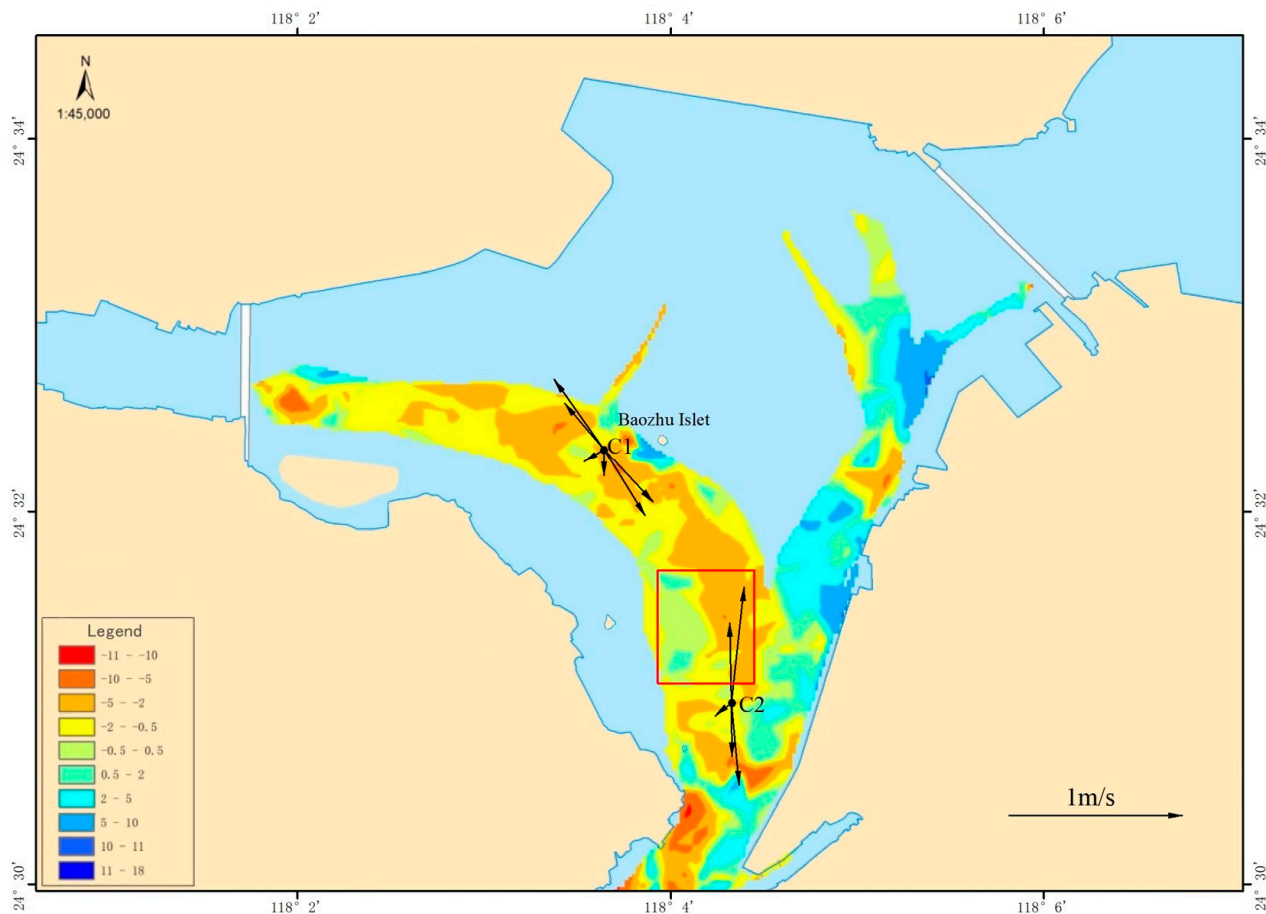


**Figure 1.** Geographical location of the Baozhu Islet Experimental Zone (red rectangle) for model launch and field exploration. Seabed stability (1999–2017) and tidal currents are also list. For seabed stability, positive value indicates erosion, negative value indicates siltation, in meters. For tidal currents, the arrows indicate the direction and velocity of the flow during spring tide, with water flowing into the bay at high tide and outside the bay at low tide.

### 2.2.2. Model Deployment

In the field experimental study, authentic ceramic flower pots manufactured locally in southern Fujian were selected to simulate underwater cultural relics, as their material composition closely resembles that of genuine artifacts. The models were categorized into three types based on size and form: small, medium, and large models. The small models consist of ceramic flower pots with a height of 10 cm and a diameter of 17 cm, arranged in clusters or strings, e.g., M2, M3 and M4 in Figure 2a. The medium models include three different sizes of ceramic flower pots: one with a height of 17 cm and a diameter of 27 cm, another with a height of 24 cm and a diameter of 33 cm, and a third with a height of 28 cm and a diameter of 38 cm, e.g., M1 in Figure 2a, M5 in Figure 2b, M6 in Figure 2c. The large model features a ceramic flower pot with a height of 70 cm and a diameter of 44 cm, as shown in Figure 2d. Based on the theoretical resolution of the sonar equipment used, we combine some of these models (as shown in Figure 2) to increase the volume of the models to enhance their recognizability on the acoustic map.

On 20 July 2022, the research team deployed a batch of ceramic flower pots of varying sizes in the Baozhu Island experimental area. The pots were arranged individually, stacked, or connected in series, and secured with thin ropes before being placed on the seafloor. Following the deployment of the models, divers conducted underwater photography to document the condition of the models on the seafloor. The state of some models after deployment on the seafloor are illustrated in Figure 3.



**Figure 2.** Physical diagram of the ceramic container. (a) Combination of medium models (M1) and small models (M2, M3, M4); (b) Combination of medium models (M5); (c) Single medium models (M6); (d) Single large models (M7).

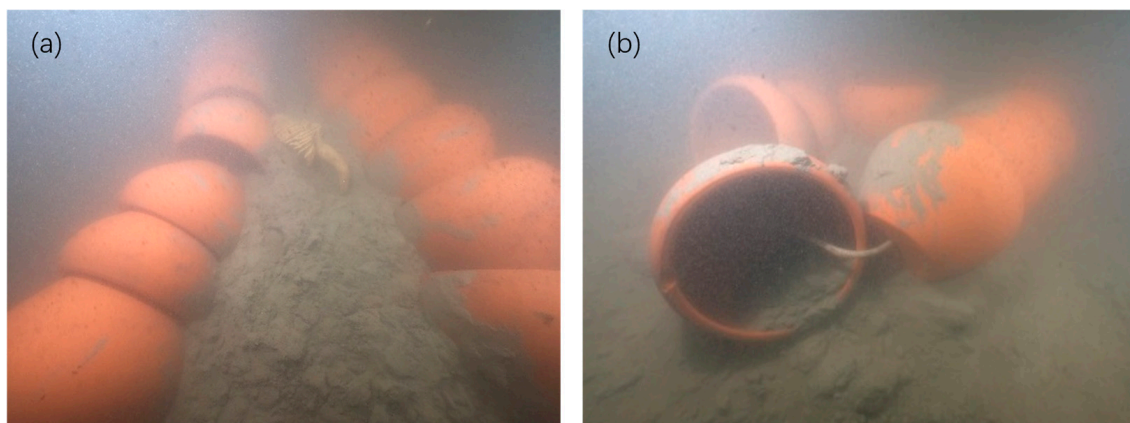


**Figure 3.** Cont.



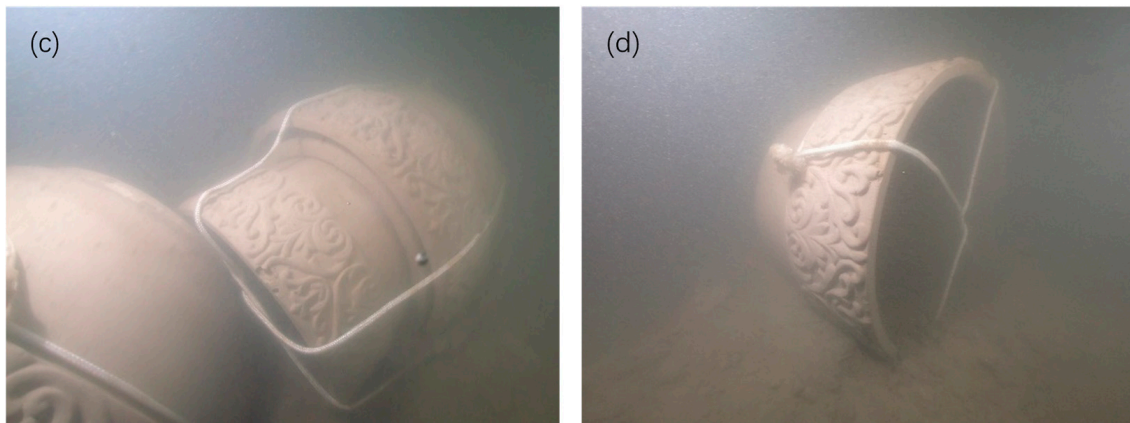


**Figure 3.** Seabed occurrence of ceramic containers. The model object is thrown from the sea surface at will and sinks to the bottom of the sea naturally. (a) M3 and M4 in Figure 2a; (b) M2 in Figure 2a; (c) M1 in Figure 2a; (d) M6 in Figure 2c.

### 2.2.3. Data Acquisition

On 20–21 July 2022, marine survey experiments were conducted based on the deployment status of the models and an assessment of the underwater conditions. The experiments included the use of MBES, SSS, and SBP system. The MBES focused on three-dimensional modeling of the seafloor topography, while the SSS was aimed at imaging underwater targets. The SBP was utilized to investigate the sedimentary environment of the experimental area. To avoid acoustic interference among these three types of instruments, separate surveys were conducted during the experiment.

Currently, commonly used MBESs typically offer various operational modes to accommodate different application scenarios, including single-frequency mode, dual-frequency mode, dynamic focusing mode, and side-scan imaging mode. The single-frequency mode employs a single frequency of sound waves for measurements, making it suitable for routine surveying tasks, characterized by high measurement speed and stability. The dual-frequency mode utilizes two different frequencies simultaneously, which is ideal for shallow water measurements, such as in ports and coastal areas, as it provides enhanced resolution and resistance to interference. The dynamic focusing mode enhances local resolution by adjusting the beam focusing area, making it suitable for shipwreck detection and detailed inspections of underwater structures. The side-scan imaging mode combines depth measurement with sonar imaging, allowing for a clear visualization of the seafloor morphology, which is particularly useful for identifying underwater pipelines, rocks, and conducting archeological surveys.

Similar to MBESs, an SSS typically offers multiple operational modes, including single-frequency and dual-frequency modes. The single-frequency mode employs a single frequency to transmit acoustic waves, making it suitable for surveying specific depths. In contrast, the dual-frequency mode utilizes two frequencies simultaneously (e.g., 150 kHz and 450 kHz), balancing broad-area scanning with high-resolution imaging, and is suitable for comprehensive exploration in both shallow- and deep-water regions, such as in the search for sunken vessels.

The acoustic impedance of ceramics, such as alumina at approximately 35 MRayl, is significantly higher than that of water (1.5 MRayl), resulting in a strong reflection of sound waves at the interface. This causes exposed ceramic objects to appear as bright targets in sonar images. Since newly deployed objects have not undergone prolonged sedimentation and are in an exposed state, they are well-suited for detection using MBES and SSS techniques.

This study employs the RESON 7125 shallow-water multibeam bathymetry sonar and the Shark-S150D dual-frequency side-scan imaging sonar to conduct field detection experiments. The RESON 7125 can be operated in three distinct modes. Some of the key technical parameters are shown in Table 1. The Shark-S150D is a versatile sonar suitable for both shallow- and deep-water measurements, equipped with dual-frequency synchronous transmission and reception at 150 kHz and 450 kHz, as well as Chirp frequency modulation processing technology. This enables both wide-area coverage and high-resolution imaging. Some key technical parameters of Shark-S150D are shown in Table 2. During the field detection process, both the MBES and SSS utilized full-coverage scanning, providing essential background data for subsequent research. The MBES employed high-density survey lines, and through post-processing, multiple survey line data were integrated to generate three-dimensional representations of topographical anomalies. Additionally, backscatter data were recorded to facilitate further investigations. Moreover, we also carried out field detection study using the SES2000 parametric sub-bottom profiler, although the models located on the surface of the seabed could not reflect the unique advantages of SBP. Some key technical parameters of SES2000 are shown in Table 3. Figure 4 shows the measurements of MBE and SSS before model deployment, showing the topography and geomorphology of the experimental sea area.

**Table 1.** Technical parameters of RESON 7125 Multibeam Echosounder System.

Pulse Frequency	200 kHz/400 kHz (Dual Frequency Available)
Pulse Type	Chirp/CW
Max Ping Rate	≤50 Hz, depend on depth
Pulse Length	30 μs–300 μs Continuous Wave; 300 μs–20 ms Frequency Modulated (X-Range)
Along-track transmit beamwidth	1°@400 kHz, 2°@200 kHz
Across-track receive beamwidth	0.5°@400 kHz, 1°@200 kHz
Number of Beams	512EA/ED at 400 kHz, 256EA/ED at 200 kHz
Max swath angle	140° in Equi-Distant Mode; 165° in Equi-Angle Mode
Max depth	0.5 m~500 m
Depth resolution	6 mm

**Table 2.** Technical parameters of Shark-S150D side-scan sonar system.

Pulse Frequency	150 kHz/450 kHz (Dual Frequency Available)
Pulse Type	Chirp/CW
Max Sweep Range	450 m@150 kHz, 150 m@450 kHz
Along-track transmit beamwidth	50°
Across-track transmit beamwidth	0.6°@150 kHz, 0.2°@450 kHz
Max Operating Depth	<2000 m
Along-track Resolution	0.01 h@150 kHz, 0.003 h@450 kHz, h equal to Max Sweep Range
Across-track Resolution	1.25 cm

**Table 3.** Technical parameters of SES2000 standard sub-bottom profiling system.

Primary Frequency	Approx. 100 kHz (Band 85–115 kHz)
Secondary Low Frequencies:	4, 5, 6, 8, 10, 12, 15 kHz (band 2–22 kHz)
Pulse Type:	CW, Ricker, LFM (chirp)
Max Ping Rate	≤60 Hz
Pulse Length	0.07~1.3 ms
Water Depth Range	1–500 m
Layer Resolution	5 cm

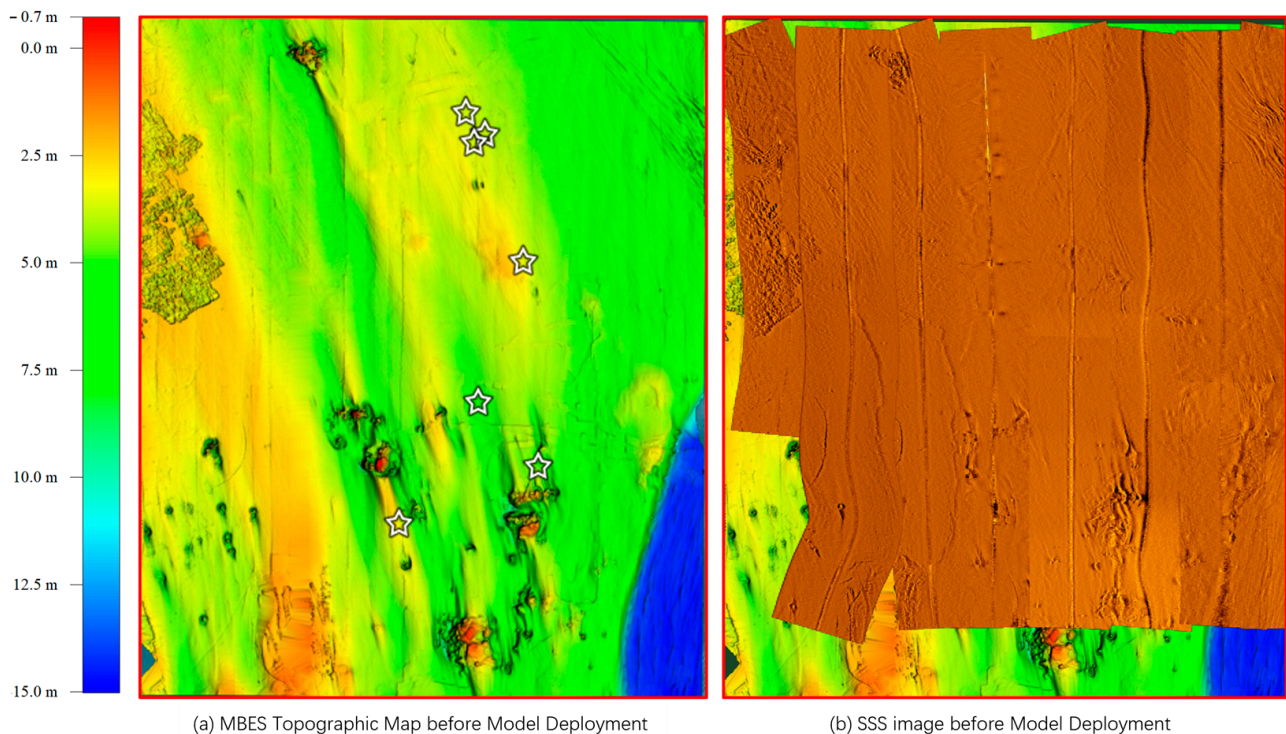


**Figure 4.** Full-coverage multibeam topographic map and SSS image of experimental (after regular processing procedure) before model deployment. The ☆ marked in this map indicates the targets' location recognized by SSS.

### 3. Results

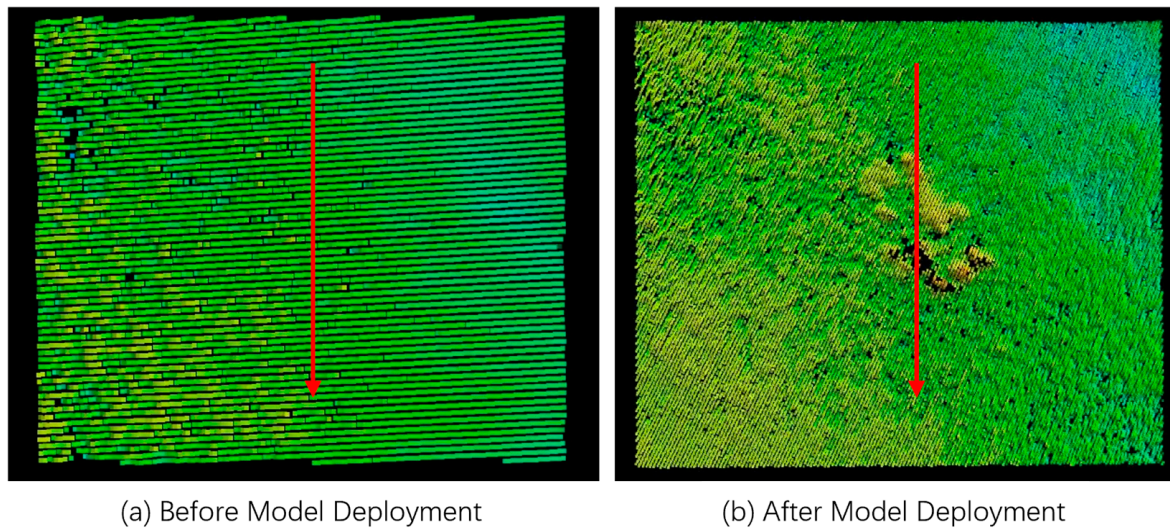
#### 3.1. Applicability of MBES

The data acquired by the RESON 7125 MBES were processed using the PDS2000 software (Version 3.9.2.3) for post-processing. Initially, the raw data underwent noise removal. Subsequently, sound speed profiles and tide level files were loaded to perform sound speed correction and tide correction. Following this, survey lines were selected and adjusted to determine the correction values for roll, pitch, and heading deviations, completing the attitude correction and yielding the bathymetric results.

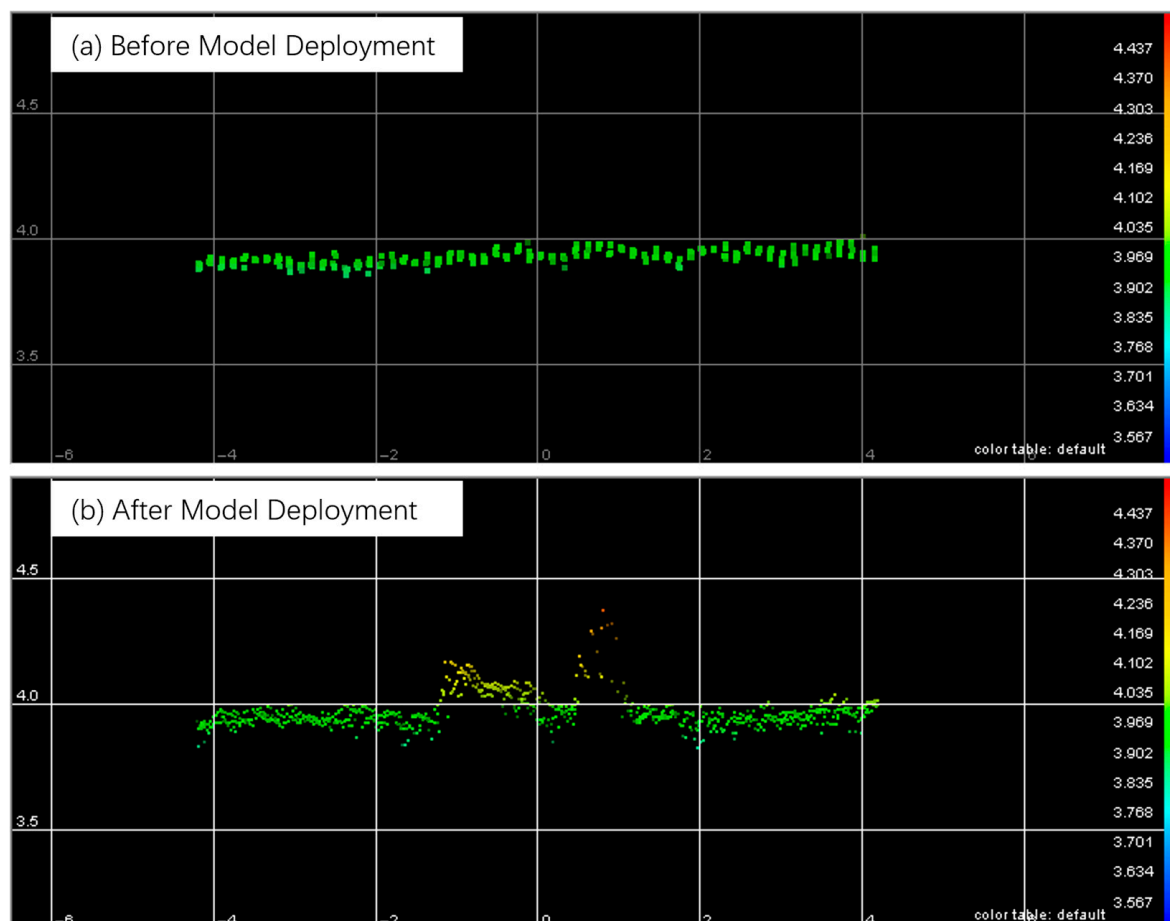
MBES data were collected in the study area both before and after the deployment of the model. A comparison of the seabed topography changes before and after deployment (Figure 5) revealed that the seabed was relatively flat prior to deployment. Following the deployment, anomalies in the seabed topography were observed, characterized by the emergence of prominent features. These features included isolated, near-elliptical mounds as well as clusters of irregularly shaped elevations. The overall shape and contours of these features were somewhat indistinct, making it difficult to discern specific details regarding their shapes and forms. It is important to note that such protrusions may be identified as isolated rocks or exposed reefs in actual marine surveys.

Figure 6 presents the topographic cross-section of the area with anomalies before and after the model deployment (as noted in Figure 5). It can be observed that prior to deployment, the topographic variation in this region did not exceed 0.1 m. Following the deployment, topographic anomalies with heights ranging from 0.3 to 0.5 m emerged, characterized by an abnormal peak shape, with localized sharp elevations. However, there is a lack of morphological details that would allow for the identification of the model type. The results of the model deployment experiments indicate that multi-beam sonar is suitable for detecting clustered artifacts or large structures; however, it lacks sufficient resolution for individual small pottery items measuring less than 30 cm.





**Figure 5.** Multi-beam topography before and after the model deployment. The red arrow indicates the section across the model object placement position, corresponding to the 2D terrain profile shown in Figures 6a,b respectively.



**Figure 6.** The terrain profile of the model before and after the model deployment. Corresponding to the two red arrow in Figure 5.

### 3.2. Applicability of SSS

Ceramic objects typically appear as high-intensity targets in underwater sonar images. In this study, SSS detection experiments were primarily conducted using the Shark-S150D

dual-frequency side-scan sonar, operating at a frequency of 150 kHz, with two different swath widths of 75 m and 90 m. In the 75 m swath width mode, at a height of 4.36 m above the seabed and a speed of 3.8 knots, the model exhibited distinct acoustic anomalies within 12.05 m (Figure 7a), although the details were not clearly defined. When the height was increased to 4.55 m and the speed to 3.9 knots, notable acoustic shadows were observed at 30.05 m (Figure 7b). In the 90 m swath width mode, at a height of 5.54 m and a speed of 3.5 knots, the model displayed significant acoustic anomalies within 12.47 m (Figure 8a), but again, the details were not prominently visible. At a height of 5.28 m and the same speed of 3.5 knots, distinct acoustic anomalies were detected at 42.47 m, although the details remained somewhat obscured (Figure 8b). Overall, the results indicate that different operational modes significantly influence the detection of target objects. Utilizing a narrower swath width and maintaining the target within an optimal detection range (between one-third and two-thirds of the swath width) can effectively enhance detection efficiency by reducing the distance between the transducer and the target.

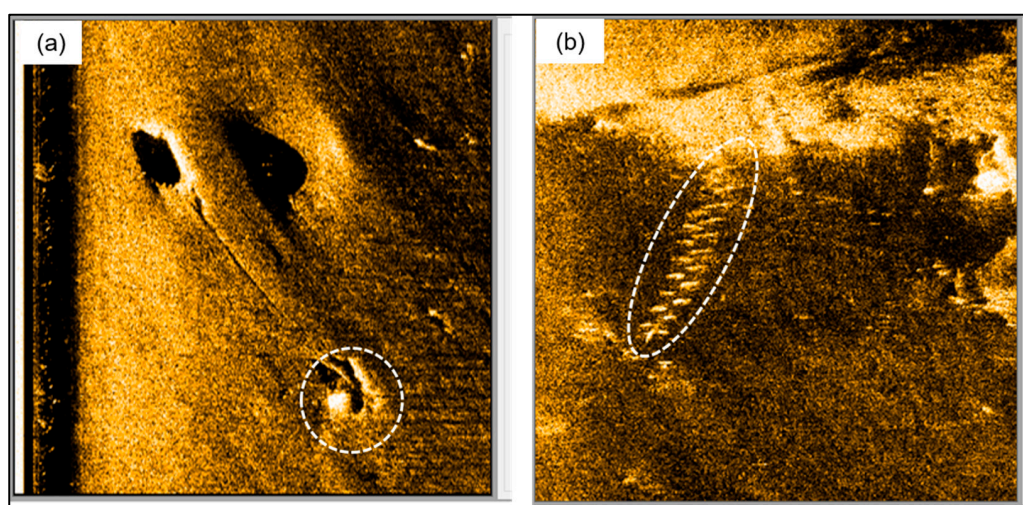


**Figure 7.** Model detection effect of Shark-S150D SSS with 75 m scan width. (a) Target #2; (b) Target #4.

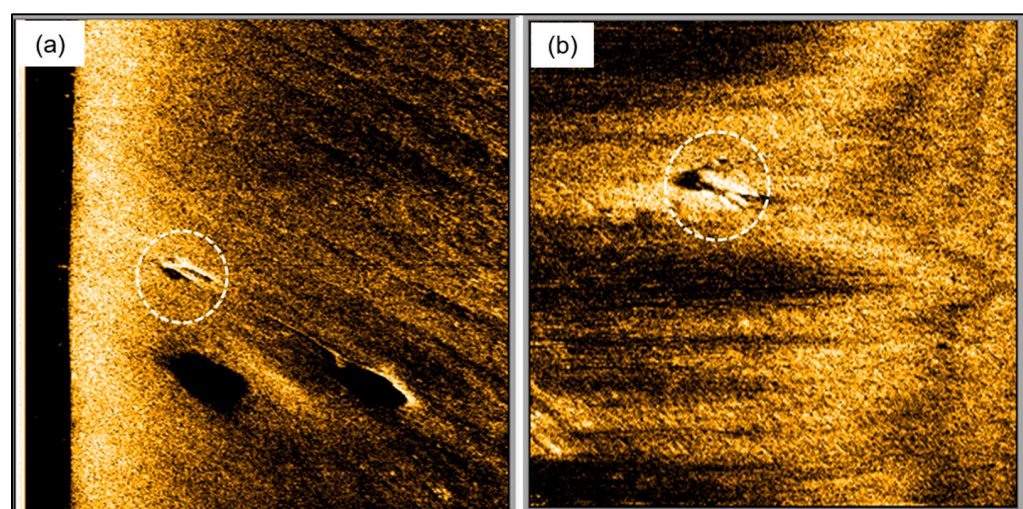


**Figure 8.** Model detection effect of Shark-S150D SSS with 90 m scan width. (a) Target #1; (b) Target #5.

The targets recognized by the SSS are indicated in the upper left portion of Figure 1, noted as “☆”. The location information is shown in Table A1, and the numbers are in the order from north to south.



### 3.3. Applicability of SBP

The primary advantage of using SBP in underwater archeology lies in its ability to detect submerged artifacts. Objects such as shipwrecks or cargo, which are non-naturally deposited, typically exhibit a significant acoustic impedance difference compared to naturally deposited sedimentary materials, particularly for materials like wood, iron, and ceramics. However, this acoustic impedance difference may diminish over time. Furthermore, when acoustic anomalies are detected on MBES or SSS images without clear outlines (such as ship shapes), SBP can be employed as a supplementary method to investigate the sedimentary environment surrounding these anomalies. This approach helps to determine whether the anomalies are isolated or if they represent outcrops of bedrock beneath the seabed.

To better simulate the actual underwater conditions of artifacts, this model detection experiment did not utilize artificial burial methods to create submerged objects but instead aimed to lay the groundwork for future research. Nevertheless, we conducted SBP experiments targeting the deployed model of interest. The SBP was primarily focused on the southern deployment site, which is located near a cluster of rocks, resulting in complex hydrodynamic conditions. It is anticipated that the deployed models will be buried underground at a relatively rapid rate in the future. However, due to the primary function of the SBP which is to penetrate the sediment layer, it can only obtain information directly beneath the transducer. Although the newly deployed ceramic models are situated on the seabed surface and exhibit a relatively high acoustic reflectivity, the profiler struggled to yield significant results. Due to the small size of the models and factors such as sea conditions and the skill level of the captain, only one survey line passed directly over the model, revealing corresponding anomalous reflection features, albeit not prominently. The applicability of SBP for deployed model detection is shown in Figure 9.

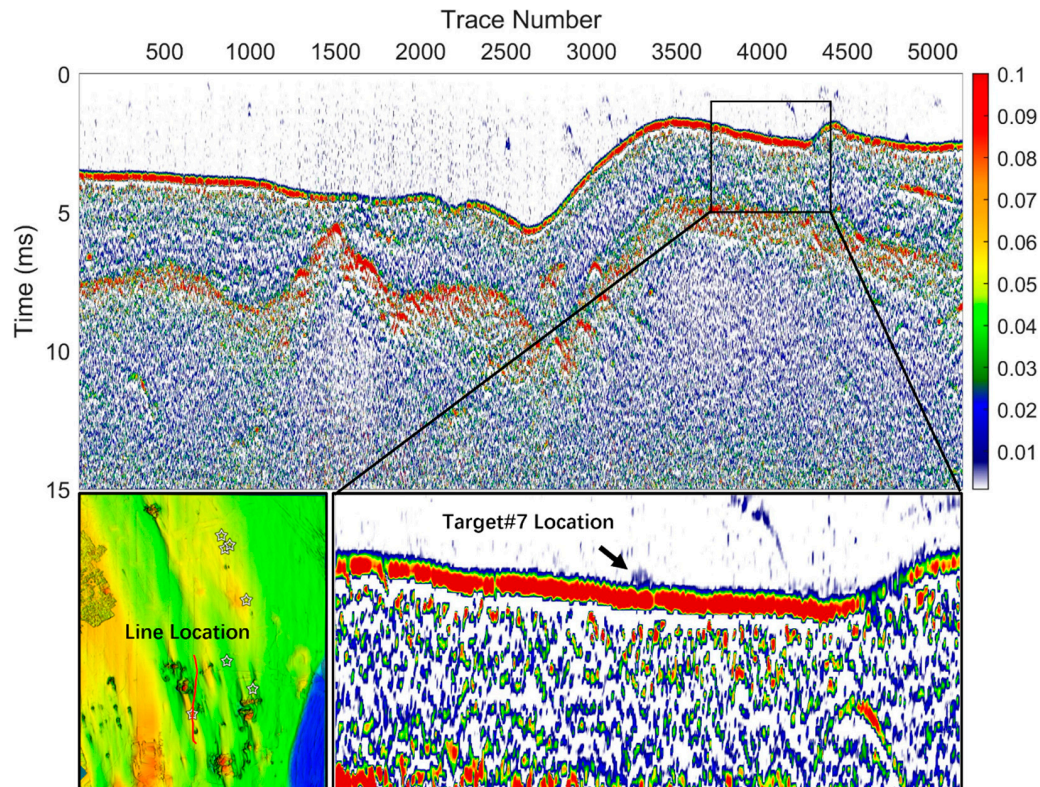


**Figure 9.** Sub-bottom profile across the deployed model near the rocks group (across Target#7).

#### 4. Discussion

The MBES offers significant advantages in three-dimensional terrain reconstruction; however, it relies on dense survey lines and sophisticated post-processing algorithms. SSS is suitable for rapid surveys but requires a reduction in vessel speed (less than 4 knots) to enhance resolution. To leverage the strengths of both methods, it is recommended to adopt a combined detection approach of “initial screening with MBES followed by detailed surveying with SSS.”

In specialized application scenarios, such as the detection of small targets, it is crucial to understand the operational mechanisms of the instruments you choose to solve problems before designing and implementing a solution. For the above acoustic sounding instruments, we think the concept of beam footprint should be kept in mind throughout the data acquisition and data processing. The beam footprint influences the resolution in the vertical track direction, while the resolution along the track direction is dependent on the survey vessel's speed and the so-called ping rate. It is important for personnel to consider the relationship between coverage and spatial resolution. For small target detection, coverage is more critical during the detection phase, whereas spatial resolution becomes more significant during the imaging phase.

The parametric array SBP exhibits notable beam focusing capabilities, resulting in a defined beam footprint. In the model detection experiment conducted, the SES2000 standard profiler was utilized, which has a nominal beam width @  $-3\text{dB}$  of  $\pm 2^\circ$ , yielding a beam footprint size of less than 7% of the water depth. In the experimental area, where the water depth is less than 10 m, this translates to a beam footprint of less than 70 cm. This characteristic is advantageous for detecting pipeline targets; however, for discontinuous targets such as isolated ceramic containers, if the transducer does not pass directly above the target, it cannot capture effective reflection characteristics of the target. This presents a technical challenge that must be addressed when using SBP for detecting small targets, especially buried isolated targets. Future studies should incorporate buried ceramic targets to assess the SBP's ability to detect relics under varying sediment conditions, as hypothesized in Section 3.3. In fact, in the absence of prior information, it is difficult to identify whether the anomalous reflection is a target from the results of SBP.

It is important to note that once a vessel or artifact sinks to the seabed, new marine environmental conditions initiate various physical, chemical, and biological processes. These include the filling of pores with moisture, corrosion, the growth of mold and algae, calcium deposition, sediment erosion, and hydrolysis. Such processes not only contribute to the corrosion and degradation of artifacts but also alter their coupling with the surrounding environment, potentially affecting their acoustic properties and other characteristics. Smooth ceramic surfaces, which have a roughness significantly smaller than the wavelength of sound waves, produce specular reflections, resulting in high echo intensity. In contrast, rough surfaces lead to scattering, which reduces echo intensity. Consequently, when the surface of a ceramic object is colonized by shellfish, it will result in a decrease in echo intensity, thereby increasing the difficulty of detection.

At present, underwater archeology in China is mainly concentrated in shallow sea areas. For acoustic surveys, in addition to the applicability of the method itself, it is also necessary to take into account the complex natural environment of the seabed and human-induced influencing factors. Different from the theoretical resolution of acoustic detection methods, conducting field experiments by deploying models in actual marine environments is significant for several reasons: (1) By deploying simulated artifacts made from various materials (such as iron, wood, and ceramics) and of different sizes (ranging from 0.1 to 5 m), we can quantitatively assess the detection limits of equipment such as SSSs and MBESs. (2) Model experiments can simulate scenarios such as shipwrecks

and ancient cities, thereby reducing the operational risks for divers in unknown areas. (3) The results of field detection experiments reveal the limitations of multi-beam sonar in identifying targets smaller than 0.5 m, highlighting the need for the development and popularization of high-resolution sonar technology. Comprehensive data analysis indicates that integrating geology (substrate analysis), oceanography (hydrological modeling), and archeology (artifact characteristics) to construct a comprehensive detection system is a crucial direction for future development.

A limitation of this study is that only ceramic models were deployed in the experimental marine area. The equipment used was relatively simple and not the most advanced available globally; however, all devices employed are common commercial equipment. Our primary objective was to investigate whether these conventional methods could be effective in scenarios where suspected small targets are present underwater, but their specific locations are unknown. We have provided the locations of certain identified models in Table A1 in Appendix A, which interested teams can reference for related experiments. It is important to note that there are additional model targets in the marine area whose locations have not been disclosed, as they could not be identified due to the limitations of the equipment's resolution in our experimental results. Future studies should utilize more advanced equipment to conduct further experiments.

## 5. Conclusions

Marine model testing serves as a bridge between technological research and practical application. By simulating detection challenges in real-world scenarios, it not only validates the feasibility of geophysical exploration techniques but also the limitation. This work aimed to provide an empirical foundation for standardized operations, risk management, and interdisciplinary collaboration. Conducted through model experiments in the Xiamen sea area, primarily reveals the applicability boundaries of MBES and SSS technologies in underwater artifact detection: (1) MBES technology is suitable for detecting clusters of artifacts or topographical anomalies but has limited capability in identifying small individual artifacts (diameter < 30 cm); (2) SSSs can effectively identify non-metallic artifacts, such as pottery, under conditions of near-bottom operation, wide swath, and low vessel speed; (3) future research should integrate laser scanning and artificial intelligence image recognition technologies to enhance the detection accuracy of small artifacts in complex environments, where the terrain changes greatly and the water flow is rapid.

**Author Contributions:** Conceptualization, J.Z. and J.X.; Data curation, Z.H.; Formal analysis, J.Z.; Funding acquisition, J.Z.; Investigation, X.F., Z.H., B.L. and P.C.; Methodology, X.F. and B.L.; Project administration, J.Z.; Resources, J.X.; Software, J.Z., S.Z. and P.C.; Supervision, J.X.; Validation, X.F.; Visualization, S.Z., B.L. and P.C.; Writing—original draft, X.F.; Writing—review and editing, J.Z. All authors have read and agreed to the published version of the manuscript.

**Funding:** This research was funded by Fujian Provincial Key Laboratory of Marine Physical and Geological Processes (KLMPG-22-04), the National Natural Science Foundation of China (NSFC: 12404546), and the National Key R&D Program of China (2020YFC1521702).

**Institutional Review Board Statement:** Not applicable.

**Informed Consent Statement:** Not applicable.

**Data Availability Statement:** Dataset available on request from the authors.

**Conflicts of Interest:** Mr. Shengtao Zhou is affiliated with Tianjin Qilan Technology Co., Ltd., and Mr. Ping Chen are affiliated with Xiamen Marine Engineering Survey, Design and Research Institute Co., Ltd. The remaining author declares that the research was conducted in the absence of any commercial or financial relationships that could be construed as a potential conflict of interest.



## Abbreviations

The following abbreviations are used in this manuscript:

MBES	Multi-beam echosounder
SSS	Side-scan sonar
SBP	Sub-bottom profiler

## Appendix A

Here we provide the model location for further study. Location information of the targets recognized by SSS is shown in Table A1. The numbers are in the order from north to south. In fact, there are more than seven targets we deployed in the experimental sea area. However, due to the limitation of the equipment we have used in this study, some of the targets did not recognize in the survey data.

**Table A1.** Location information of the ceramic models.

Target Number	Longitude	Latitude
#1	118°04.2435' E	24°31.5347' N
#2	118°04.2573' E	24°31.5127' N
#3	118°04.2505' E	24°31.5276' N
#4	118°04.2926' E	24°31.4246' N
#5	118°04.2530' E	24°31.2847' N
#6	118°04.3067' E	24°31.2466' N
#7	118°04.1785' E	24°31.1987' N

## References

- Li, Y.; Wen, M.; Chen, Z.; Yao, H.; Wan, P.; Li, B.; Lin, H.; Chen, Z. Advance, challenge, and suggestion in geophysical technology for underwater archaeology survey. *Mar. Geol. Quat. Geol.* **2023**, *43*, 191–201.
- Menna, F.; Agrafiotis, P.; Georgopoulos, A. State of the art and applications in archaeological underwater 3D recording and mapping. *J. Cult. Herit.* **2018**, *33*, 231–248. [\[CrossRef\]](#)
- Violante, C.; Gallochio, E.; Pagano, F.; Papadopoulos, N. Geophysical and geoarchaeological investigations in the Submerged Archeological Park of Baia. In Proceedings of the 2023 IMEKO TC-4 International Conference on Metrology for Archaeology and Cultural Heritage, Rome, Italy, 19–21 October 2023.
- Quinn, R.; Bull, J.M.; Dix, J.K. Imaging wooden artefacts using Chirp sources. *Archaeol. Prospect.* **1997**, *4*, 25–35. [\[CrossRef\]](#)
- Grøn, O.; Boldreel, L.O. Sub-bottom profiling for large-scale maritime archaeological survey: An experience-based approach. In Proceedings of the 2013 MTS/IEEE OCEANS—Bergen, Bergen, Norway, 10–14 June 2013.
- Grøn, O.; Boldreel, L.O.; Cvikel, D.; Kahanov, Y.; Galili, E.; Hermand, J.-P.; Nævestad, D.; Reitan, M. Detection and mapping of shipwrecks embedded in sea-floor sediments. *J. Archaeol. Sci. Rep.* **2015**, *4*, 242–251. [\[CrossRef\]](#)
- Grøn, O.; Jorgensen, A.N.; Hoffmann, G. Marine archaeological survey by high-resolution sub-bottom profilers. In *Norsk Sjøfartsmuseums Årbok 2007*; pp. 115–145. Available online: <https://www.mendeley.com/catalogue/9ff0b89c-c51b-3ca0-b8e4-d2eaf4ba8c7e/> (accessed on 14 September 2025).
- Wunderlich, J.; Wendt, G.; Müller, S. High-resolution Echo-sounding and Detection of Embedded Archaeological Objects with Nonlinear Sub-bottom Profilers. *Mar. Geophys. Res.* **2005**, *26*, 123–133. [\[CrossRef\]](#)
- Plets, R.M.K.; Dix, J.K.; Adams, J.R.; Best, A.I. 3D reconstruction of a shallow archaeological site from high-resolution acoustic imagery: The Grace Dieu. *Appl. Acoust.* **2008**, *69*, 399–411. [\[CrossRef\]](#)
- Plets, R.M.K.; Dix, J.K.; Adams, J.R.; Bull, J.M.; Henstock, T.J.; Gutowski, M.; Best, A.I. The use of a high-resolution 3D Chirp sub-bottom profiler for the reconstruction of the shallow water archaeological site of the Grace Dieu (1439), River Hamble, UK. *J. Archaeol. Sci.* **2009**, *36*, 408–418. [\[CrossRef\]](#)
- Missiaen, T. The potential of seismic imaging in marine archaeological site investigations. *Relicta* **2010**, *6*, 219–236. [\[CrossRef\]](#)
- Mueller, C.; Woelz, S.; Kalmring, S. High-Resolution 3D Marine Seismic Investigation of Hedeby Harbour, Germany. *Int. J. Naut. Archaeol.* **2013**, *42*, 326–336. [\[CrossRef\]](#)
- Castillón, M.; Palomer, A.; Forest, J.; Ridao, P. State of the Art of Underwater Active Optical 3D Scanners. *Sensors* **2019**, *19*, 5161. [\[CrossRef\]](#)
- Bräuer-Burchardt, C.; Munkelt, C.; Bleier, M.; Heinze, M.; Gebhart, I.; Kihmstedt, P.; Notni, G. Underwater 3D Scanning System for Cultural Heritage Documentation. *Remote. Sens.* **2023**, *15*, 1864. [\[CrossRef\]](#)

15. Yang, Y.; Liang, W.; Zhou, D.; Zhang, Y.; Xu, G. Object Detection for Underwater Cultural Artifacts Based on Deep Aggregation Network with Deformation Convolution. *J. Mar. Sci. Eng.* **2023**, *11*, 2228. [\[CrossRef\]](#)
16. Davis, D.S.; Buffa, D.; Wroblewski, A.C. Assessing the Utility of Open-Access Bathymetric Data for Shipwreck Detection in the United States. *Heritage* **2020**, *3*, 364–383. [\[CrossRef\]](#)
17. Westley, K. Satellite-derived bathymetry for maritime archaeology: Testing its effectiveness at two ancient harbours in the Eastern Mediterranean. *J. Archaeol. Sci. Rep.* **2021**, *38*, 103030. [\[CrossRef\]](#)
18. Ntuli, S.; Akombelwa, M.; Forbes, A.; Singh, M. Classification of 3D Sonar Point Clouds derived Underwater using Machine and Deep Learning (CANUPO and RandLA-Net) Approaches. *S. Afr. J. Geomatics* **2024**, *13*, 269–287. [\[CrossRef\]](#)
19. Abate, N.; Violante, C.; Masini, N. A Semi-Automatic-Based Approach to the Extraction of Underwater Archaeological Features from Ultra-High-Resolution Bathymetric Data: The Case of the Submerged Baia Archaeological Park. *Remote Sens.* **2024**, *16*, 1908. [\[CrossRef\]](#)
20. Quinn, R.; Adams, J.R.; Dix, J.K.; Bull, J.M. The Invincible (1758) site—An integrated geophysical assessment. *Int. J. Naut. Archaeol.* **1998**, *27*, 126–138.
21. Quinn, R.; Breen, C.; Forsythe, W.; Barton, K.; Rooney, S.; O'Hara, D. Integrated Geophysical Surveys of The French Frigate La Surveillante (1797), Bantry Bay, Co. Cork, Ireland. *J. Archaeol. Sci.* **2002**, *29*, 413–422. [\[CrossRef\]](#)
22. Jaijel, R.; Glover, J.B.; Rissolo, D.; Beddows, P.A.; Smithe, D.; Ben-Avraham, Z.; Goodman-Tchernova, B. Coastal reconstruction of Vista Alegre, an ancient maritime Maya settlement. *Palaeogeogr. Palaeoclimatol. Palaeoecol.* **2018**, *497*, 25–36. [\[CrossRef\]](#)
23. Jaijel, R.; Kanari, M.; Glover, J.B.; Rissolo, D.; Beddows, P.A.; Ben-Avraham, Z.; Goodman-Tchernov, B.N. Shallow geophysical exploration at the ancient maritime Maya site of Vista Alegre, Yucatan Mexico. *J. Archaeol. Ence Rep.* **2018**, *19*, 52–63. [\[CrossRef\]](#)
24. Bingham, B.; Foley, B.; Singh, H.; Camilli, R.; Delaporta, K.; Eustice, R.; Mallios, A.; Mindell, D.; Roman, C.; Sakellariou, D. Robotic tools for deep water archaeology: Surveying an ancient shipwreck with an autonomous underwater vehicle. *J. Field Robot.* **2010**, *27*, 702–717. [\[CrossRef\]](#)
25. Xanthidis, M.; Joshi, B.; O'Kane, J.; Rekleitis, I.M. Multi-Robot Exploration of Underwater Structures. *IFAC-PapersOnLine* **2022**, *55*, 395–400. [\[CrossRef\]](#)

**Disclaimer/Publisher's Note:** The statements, opinions and data contained in all publications are solely those of the individual author(s) and contributor(s) and not of MDPI and/or the editor(s). MDPI and/or the editor(s) disclaim responsibility for any injury to people or property resulting from any ideas, methods, instructions or products referred to in the content.